Available online at www.sciencedirect.com
ScienceDirect
Journal of Controlled Release 122 (2007) 365–374
journal of controlled release
www.elsevier.com/locate/jconrel

β-Lapachone-containing PEG–PLA polymer micelles as novel nanotherapeutics against NQO1-overexpressing tumor cells

Elvin Blanco [a], Erik A. Bey [a], Ying Dong [a], Brent D. Weinberg [b], Damon M. Sutton [a], David A. Boothman [a], Jinming Gao [a,*]

[a] *Simmons Comprehensive Cancer Center, University of Texas Southwestern Medical Center at Dallas, Dallas, TX 75390, United States*
[b] *Department of Biomedical Engineering, Case Western Reserve University, Cleveland, Ohio 44106, United States*

Received 24 February 2007; accepted 19 April 2007
Available online 29 April 2007

Abstract

β-Lapachone (β-lap) is a novel anticancer agent that is bioactivated by NADP(H): quinone oxidoreductase 1 (NQO1), an enzyme overexpressed in a variety of tumors. Despite its therapeutic promise, the poor aqueous solubility of β-lap hinders its preclinical evaluation and clinical translation. Our objective was to develop β-lap-containing poly(ethylene glycol)-block-poly(D,L-lactide) (PEG–PLA) polymer micelles for the treatment of NQO1-overexpressing tumors. Several micelle fabrication strategies were examined to maximize drug loading. A film sonication method yielded β-lap micelles with relatively high loading density (4.7±1.0% to 6.5±1.0%) and optimal size (29.6±1.5 nm). Release studies in phosphate-buffered saline (pH 7.4) showed the time ($t_{1/2}$) for 50% of drug release at 18 h. In vitro cytotoxicity assays were performed in NQO1-overexpressing (NQO1+) and NQO1-null (NQO1−) H596 lung, DU-145 prostate, and MDA-MB-231 breast cancer cells. Cytotoxicity data showed that after a 2 h incubation with β-lap micelles, a marked increase in toxicity was shown in NQO1+ cells over NQO1− cells, resembling free drug both in efficacy and mechanism of cell death. In summary, these data demonstrate the potential of β-lap micelles as an effective therapeutic strategy against NQO1-overexpressing tumor cells.

Keywords: β-Lapachone; Polymer micelles; Cancer nanomedicine; Poly(ethylene glycol)–poly(D,L-lactide) (PEG–PLA); Drug delivery

1. Introduction

Presently, the development of integrated cancer nanomedicine, which consists of drugs that exploit cancer-specific molecular targets combined with effective carriers for tumor-targeted drug delivery, has shown significant promise in expanding therapeutic indices for chemotherapy. β-Lapachone (β-lap) (Fig. 1A) is a novel, plant-derived anticancer drug whose cytotoxic effect is significantly enhanced by NAD(P)H: quinone oxidoreductase 1 (NQO1), a flavoprotein found overexpressed (up to 20-fold) in a variety of human cancers, including those of the lung [1], prostate [2], pancreas [3], and breast [4]. Upon β-lap administration, NQO1 induces a futile cycling of β-lap, wherein the compound cycles between its hydroquinone, semiquinone, and quinone forms, depleting the cell of NAD(P)H in the process and leading to the generation of DNA damaging hydroxyl radicals [5]. Additionally, β-lap treatment leads to an NQO1-dependent rise in cytosolic Ca^{2+} that results in the loss of mitochondrial membrane potential, ATP depletion, unique substrate proteolysis, DNA fragmentation, and cell apoptosis [6]. The mechanism of action is independent of caspases, p53 status, and cell cycle stage [7]. Given its central role in β-lap-mediated lethality, NQO1 is a vital, exploitable target for the treatment of cancer cells that overexpress this enzyme.

While β-lap proves to be a very promising agent from a pharmacodynamic standpoint, several factors hinder conventional intravenous administration for preclinical evaluation and clinical translation. Firstly, its non-specific distribution can lead to low tumor concentrations and systemic toxicity [8]. Moreover, its polycyclic nature makes it highly hydrophobic,

* Corresponding author. Tel.: +1 214 648 9278; fax: +1 214 648 0264.
E-mail address: jinming.gao@utsouthwestern.edu (J. Gao).

0168-3659/$ - see front matter © 2007 Elsevier B.V. All rights reserved.
doi:10.1016/j.jconrel.2007.04.014

with an aqueous solubility of 0.04 mg/mL [9]. Prior work by our laboratory focused on attempts to increase the aqueous solubility of β-lap through its complexation with hydroxypropyl-β-cyclodextrin (HPβ-CD) [9]. However, the fast dissociation of β-lap and cyclodextrin makes the drug susceptible to aggregation and rapid clearance, warranting the use of an effective nanotherapeutic delivery vehicle that can efficiently solubilize the drug and deliver it to solid tumors.

Polymer micelles are spherical, nanosized (10–100 nm) supramolecular constructs that are garnering significant attention as a versatile drug delivery platform for cancer therapy [10–12]. Polymer micelles have a unique core-shell structure as a result of the self-assembly of amphiphilic block copolymers in aqueous environments (Fig. 1B). The hydrophobic core acts as a solubilizing reservoir for water insoluble drugs, such as β-lap, providing protection from enzymatic degradation and inactivation [13]. The hydrophilic micellar corona, in turn, forms a hydrating layer on the surface of the micelle that hinders plasma protein adsorption and subsequent rapid phagocytic clearance by the reticuloendothelial system (RES) [14]. Additionally, small micellar size, along with low critical micelle concentrations (CMCs), results in long-circulating, stable constructs that do not easily dissociate in vivo [15], and contributes to the preferential accumulation of micelles in tumor tissue through the enhanced permeability and retention (EPR) effect [16,17].

To exploit these numerous advantages of polymer micelles, our objective was to develop β-lap-containing micelles for an NQO1-specific therapy. In this study, we report the development of a film sonication method to fabricate β-lap micelles with relatively high loading of the drug, adequate micelle size, core-shell formation, and favorable release characteristics. Using three different cancer cell lines, β-lap micelle treatment showed a substantial increase in cytotoxicity in NQO1+ cells over NQO1− cells, highlighting the system as a potential treatment strategy against NQO1-overexpressing tumors.

2. Materials and methods

2.1. Materials

β-lap was synthesized following a previously reported procedure [18]. PEG5k–PLA5k block copolymer (Mn=10,000 Da) was synthesized utilizing a ring-opening polymerization procedure published previously [19]. Poly(D,L-lactide) (PLA) (Mn=27,344 Da) was purchased from Birmingham Polymers (Pelham, AL). All organic solvents were of analytical grade. H596 non-small cell lung carcinoma (NSCLC) cells, DU-145 prostate, and MDA-MB-231 breast cancer cells, were grown in DMEM with 10% fetal bovine serum, 2 mM L-glutamine, 100 units/mL penicillin, and 100 mg/mL streptomycin at 37 °C in a humidified incubator with a 5% CO_2–95% air atmosphere. All cells were routinely found free of mycoplasma infection.

2.2. β-Lap micelle fabrication

Three distinct micelle preparation methods (dialysis, solvent evaporation, film sonication) were used to encapsulate β-lap within PEG–PLA micelles. For all preparation methods a 10% theoretical loading (e.g. 1 mg of β-lap and 9 mg of PEG–PLA diblock copolymer) was used unless otherwise stated. In the dialysis method, the drug and polymer were dissolved in acetone, placed within a dialysis bag (MW cutoff=2000 Da), and dialyzed against water overnight at 4 °C. The solvent evaporation method consisted of dissolving β-lap and PEG–PLA in acetone and adding the mixture dropwise to water under sonication by a Fisher Scientific Sonic Dismembrator 60 (Hampton, NH) with an output power of 0.010 W, after which the solvent was allowed to evaporate overnight. Finally, the film sonication procedure involved the dissolution of β-lap and PEG–PLA in acetone and evaporation of the solvent, yielding a solid film. Water was then added to the film and sonicated for 5 min. In each case, drug-loaded polymer micelles were filtered through 0.45 μm nylon filters to remove non-encapsulated drug aggregates in solution, and all micelle preparations above were stored immediately at 4 °C to hinder premature drug release.

Drug loading was determined using a method previously established by Shuai et al. [19]. Briefly, 0.5 mL of micelle solution was centrifuged at a rotational speed of 2000 RPM for 30 min at 4 °C (Eppendorf Centrifuge 5804 R) using Amicon Ultra Centrifugal Filter Devices (MW cutoff=100,000 Da). Absorbance of β-lap in the resulting filtrate was measured (λ_{max}=257.2 nm, ε=105 mL/(cm·mg β-lap) using a Perkin

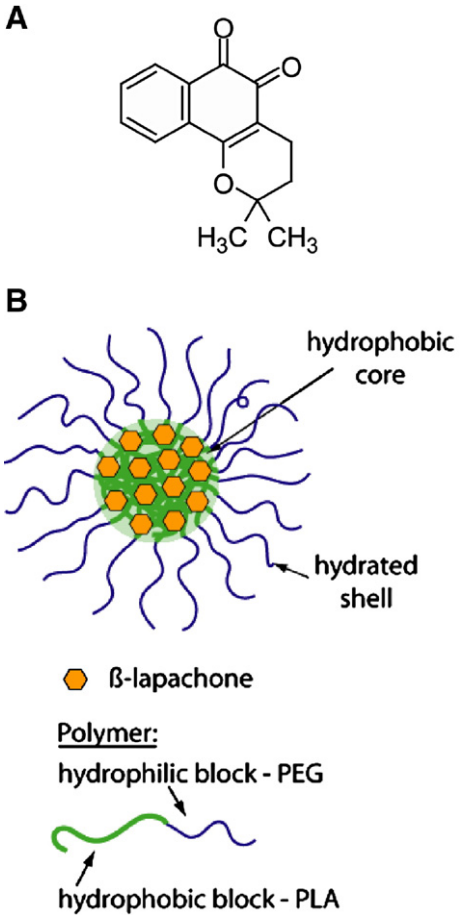

Fig. 1. (A) Chemical structure of β-lap (MW=242 Da). (B) Schematic of a β-lap-containing polymer micelle and constituent components.

Elmer Lambda 20 UV–Vis Spectrophotometer (Fremont, CA). Micelle solutions were then lyophilized overnight and the resulting freeze-dried powder was accurately weighed, dissolved in chloroform, and analyzed via UV–Vis spectrophotometry to provide the total amount of β-lap (free and micelle encapsulated). Yield, loading efficiency, and loading density of β-lap were then determined utilizing the following set of equations:

$$\%\ \text{yield} = \frac{\text{total micelle amount} - \text{free } \beta\text{-lap amount}}{\text{theoretical total micelle amount}} \times 100 \quad (1)$$

$$\%\ \text{drug loading efficiency} = \frac{\text{amount } \beta\text{-lap in micelles}}{\text{initial amount of } \beta\text{-lap in system}} \times 100 \quad (2)$$

$$\%\ \text{drug loading density} = \frac{\text{amount } \beta\text{-lap in micelles}}{\text{amount of micelles} - \text{free } \beta\text{-lap}} \times 100 \quad (3)$$

Micelle fabrication experiments were conducted in triplicate and following data tabulation, statistical analyses between different groups were performed using a Student's two-tailed *t*-test ($P<0.05$).

2.3. Differential scanning calorimetry (DSC) analysis

DSC measurements of the solid-state solubility of β-lap in PLA were performed using a Shimadzu Differential Scanning Calorimeter (DSC-60, Columbia, USA) with samples under a nitrogen atmosphere. The procedure was adapted from a method published by Panyam et al. [20] and previously utilized by our laboratory to determine the solid-state solubility of β-lap in poly(D,L-lactide-co-glycolide) (PLGA) [21]. Briefly, known quantities of β-lap (13 mg) and PLA (27.8 mg) were separately dissolved in acetone. Different amounts of drug were mixed with polymer, and transferred to aluminum pans. The solvent was then evaporated, and pans were crimped and weighed. Samples were heated to 180 °C at a rate of 10 °C/min. The heats of melting of β-lap were obtained using the peak integration calculation method provided by the DSC software. The solid-state solubility value of β-lap was determined by plotting enthalpy values as a function of the percentage of β-lap loading. The *X*-intercept resulting from a linear regression of the data represents the solid-state solubility value of β-lap in PLA.

2.4. β-Lap micelle characterization

Following fabrication, micelle size was determined using a Viscotek Dynamic Light Scattering (DLS) instrument (Houston, TX). Scattered light was detected at a 90° angle. Data was obtained from 10 measurements of 5 s duration and averaged utilizing the instrumental software to determine micelle size and size distribution.

Micelles were analyzed by ^{1}H NMR to verify core-shell architecture. β-Lap-loaded PEG–PLA micelles were prepared using the film sonication technique at 10% w/w theoretical drug loading. Following micelle fabrication and filtration, the micelle solution was split among two Amicon Ultra Centrifugal Filter Devices (MW cutoff=100,000 Da) and concentrated by centrifugation at a speed of 2000 RPM at 4 °C to minimize premature drug loss. Micelles were then washed with water to remove free drug. Once the absorbance of both supernatants was well below a value of 0.1, micelles were freeze-dried. One batch of micelles was resuspended in D_2O, while another batch was dissolved in deuterated chloroform. The two samples were then analyzed utilizing a 400-MHz Varian NMR spectrometer (Palo Alto, CA) and the resulting spectra were compared to spectra obtained from β-lap dissolved in D_2O and PEG–PLA dissolved in chloroform.

Release studies of β-lap-containing PEG–PLA micelles were performed to examine β-lap release kinetics. Approximately 100 mg of β-lap-loaded polymer micelles were prepared utilizing the film sonication technique at a theoretical loading of 10% w/w. After micelle fabrication, the amount of loaded drug and micelles was determined, and equal amounts of micelles were aliquoted among Spectrum Float-A-Lyzer dialysis devices with a molecular weight cutoff of 100,000 Da. Release studies were conducted in triplicate in PBS at a pH of 7.4 at 37 °C. At predetermined times, the buffer solution (12 mL) was removed and replaced with an equal amount of fresh buffer solution. The amount of β-lap released from micelles was determined by measuring the absorbance of the dialysis medium at 257.2 nm via UV–Vis spectrophotometry.

2.5. Modeling of β-lap release kinetics from micelles

Theoretical models were developed to simulate the drug release profiles from polymer micelles. Previous work has shown that drug release from a micelle core occurs in two successive stages: early release that can be well described by a Higuchi dissolution model (Eqs. (4) and (5)) and late release that is well approximated by Fickian diffusion (Eq. (6)) [22]:

$$\frac{M(t)}{M(\infty)} = 1 - \left[\left(\frac{\alpha'}{\alpha_0}\right)^3 + \frac{1}{2}\frac{c_s}{c_0}\left(\left(\frac{\alpha'}{\alpha_0}\right) + \left(\frac{\alpha'}{\alpha_0}\right)^2 - 2\left(\frac{\alpha'}{\alpha_0}\right)^3\right)\right] \quad (4)$$

$$c_0\left(\alpha_0^3 + 2\alpha'^3 - 3\alpha_0\alpha'^2\right) + c_s\left(4\alpha'^2\alpha_0 + \alpha_0^3 \ln\frac{\alpha_0}{\alpha'} - \alpha_0^3 - \alpha_0^2 a' - 2\alpha'^3\right) = 6Dc_s a_0 t \quad (5)$$

$$\frac{M(t)}{M(\infty)} = p\left(1 - \frac{6}{\pi^2}\exp\left(\frac{-\pi^2 Dt}{a_0^2}\right)\right) \quad (6)$$

where $M(t)$ is the mass of drug released at time t and $M(\infty)$ is the amount of drug released as time approaches infinity. The Higuchi model approximates drug release as a steadily moving front of dissolving drug moving inward from the periphery of the micelle core, where the drug is contained [23]. This model

has five parameters: the radius of the micelle core, a_0; the distance of the moving front from the center of the core at time t, a'; the initial micelle drug loading, c_0; the solubility of drug in solution, c_s; and the diffusivity of the drug in the micelle core, D_h. Later drug release was shown to be correctly approximated by Fickian diffusion out of a sphere, which has three parameters: the fraction of the drug released at infinite time, p_0; the radius of the micelle core, a_0; and the diffusivity of drug in the micelle core, D_f [24,25]. β-Lap solubility and micelle loading were known: c_s=0.04 mg/mL and c_0=8.68 mg/mL. The radius of gyration of the 5 kD PEG corona (6.16 nm) was subtracted from the hydrodynamic micelle radius (14.6 nm) to determine the size of the micelle core, a_0=8.44 nm, as reported previously [22]. The drug released by 360 h was used as the drug released at infinite time, p_0. Estimates of the two remaining unknowns, the rates of β-lap diffusion, D_h and D_f, were then calculated using non-linear least squares parameter estimation (Matlab 7.1). D_h and D_f were estimated using release data from 0–18 and 18–360 h, respectively.

2.6. Cytotoxicity of β-lap micelles in vitro

Relative survival assays based on DNA content were performed in three different cancer cell lines with isogenic expression (or inhibition of enzyme activities with dicoumarol) of NQO1 as previously described [5]. H596 non-small cell lung cancer and MDA-MB-231 breast cancer cells contain homozygous *2 NQO1 polymorphisms and thereby lack NQO1 expression. Isogenic NQO1+ counterparts were generated and characterized for β-lap free drug responses as described [5,26]. In contrast, DU-145 human prostate cancer cells endogenously over-express NQO1, and its enzyme activity can be blocked by coadministration of dicoumarol, mimicking an NQO1-deficient cell. Briefly, NQO1+ or NQO1− H596 and MDA-MB-231 cells were seeded (10,000 cells/well) into each well of 48-well plates. DU-145 cells were seeded similarly. On the following day, media were removed, and media containing predetermined doses of free β-lap drug (dissolved in DMSO) or β-lap micelles (prepared via the film sonication method) were added for a duration of 2 h. For DU-145 cells, dicoumarol at a concentration of 40 μM was coadministered to cells to inhibit NQO1. After 2 h exposures, media were then removed, control growth media added, and cells were allowed to grow for an additional 7 days. DNA content was determined by DNA fluorescence Hoescht dye 33258, using an adaptation of the method of Labarca and Paigen [27]. Samples were read in a Perkin Elmer HTS 7000 Bio Assay Reader (Waltham, MA) and data were expressed as means±SE relative growth and graphed as treated/control (T/C) values from six wells per treatment.

Table 1
β-Lapachone micelle size, yield, and drug loading parameters from different fabrication procedures

Micelle fabrication method	Theoretical loading (%)	Micelle size (nm)	Yield (%)	Loading efficiency (%)	Loading density (%)
Dialysis	10	23.3±1.2	36.3±3.4	0.08±0.04	0.02±0.01
Solvent evaporation	10	17.3±0.2	95.0±1.8	4.1±0.6	0.4±0.1
Film sonication	5	28.4±2.7	88.6±3.7	39.8±1.0	2.2±0.1
	10	29.6±1.5	85.3±6.7	41.9±5.6	4.7±1.0
	20	26.8±3.2	85.2±3.0	32.9±5.9	6.5±1.0

2.7. DNA damage and cell death assays

Distinct biological assays were conducted in NQO1+ and NQO1− H596 cells to corroborate the mechanism of action of β-lap-mediated cell death via micellar drug delivery versus responses known for free drug [7,26,28,29]. The first consisted of reactive oxygen species (ROS) analyses. Following β-lap micelle exposure to cells, ROS formation was ascertained using the conversion of non-fluorescent 5, 6-Chloromethyl-2V, 7V-dichlorodihydrofluorescein diacetate (CM-H_2DCFDA) to its fluorescent derivative (DCF) by flow cytometry (FC-500 flow cytometer, Beckman Coulter Electronics, Miami, FL) as described [30].

DNA damage analyses, or alkaline comet assays, were also performed. DNA lesions, including DNA single and double strand breaks (SSBs, DSBs, respectively), as well as DNA base damage, were assessed in single cells treated with β-lap micelles using alkaline comet assays as previously described [28,31]. Slides were stained with SYBR-green and visualized using a Nikon Eclipse TE2000-E fluorescence microscope (Melville, NY), after which digital photomicrographs were taken.

Lastly, nucleotide analyses were conducted, where changes in intracellular nicotinamide adenine dinucleotide (NAD+) levels were measured in cells after β-lap micelle exposure as described [28]. Intracellular NAD+ levels were expressed as percentage of treated divided by control (%T/C).

3. Results

3.1. Effect of different micelle fabrication methods on drug loading

Several different micelle fabrication techniques were examined with the purpose of generating β-lap micelles with an adequate size, yield, and drug loading density and efficiency. Table 1 depicts the size, yield, and loading values obtained from the three different fabrication methods. As shown in the table, from an initial 10% theoretical loading, the dialysis method produced micelles with an extremely low drug loading at 0.02±0.01%, as well as a poor loading efficiency (0.08±0.04%) and micelle yield (36.3±3.40%). The solvent evaporation procedure provided a marked improvement in β-lap loading over the dialysis method, with a loading percentage of 0.39±0.05%, but with a low loading efficiency of 4.12±0.64%. Conversely, the film sonication method produced the highest β-lap loading of micelles among all three fabrication methods, with a 4.7±1.0% drug loading at a theoretical loading of 10%, a loading efficiency of 41.9±5.6%, and a high micelle yield of 85.3±6.7%. With a subsequent increase in theoretical drug loading to 20%, β-lap loading in micelles increased to 6.5±1.0%.

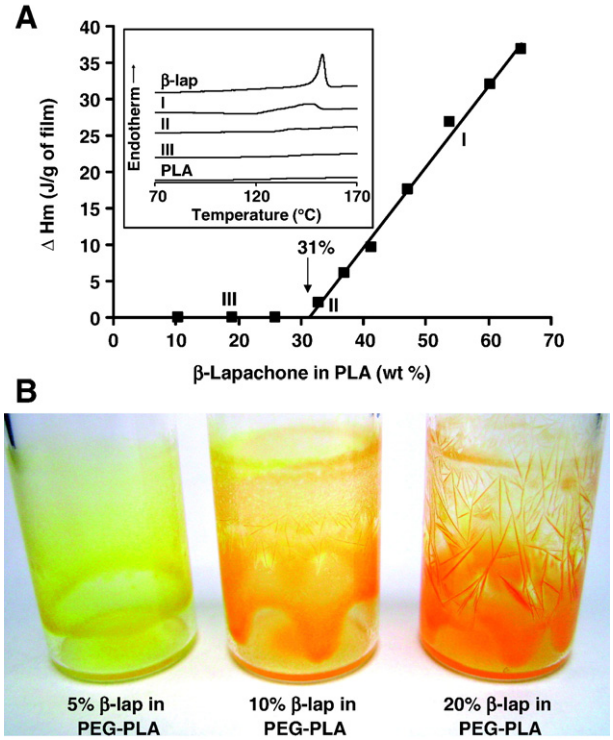

Fig. 2. Solid-state solubility studies of β-lap in PLA polymer. Fig. 2A depicts β-lap melting enthalpy (ΔH_m) as a function of β-lap loading percentage. The *X*-intercept indicates the solubility limit of β-lap in PLA. Fig. 2B represents images of β-lap and PLA films at different loading percentages for qualitative comparison.

Meanwhile, a lowered loading efficiency to 32.9±5.9% was observed at this composition. Taken together, these data highlight the effectiveness of the film sonication method at producing higher loaded β-lap micelles over other micelle fabrication methods, with differences in loading percentage values being statistically significant ($P<0.05$).

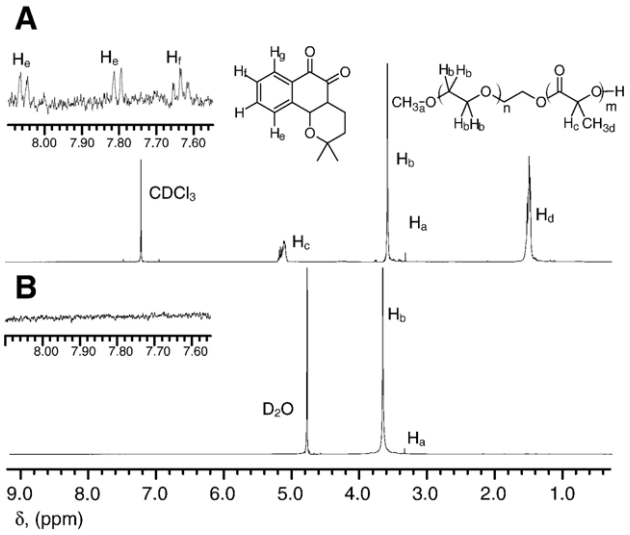

Fig. 3. ^{1}H NMR spectra of β-lap-loaded PEG–PLA micelles in (A) deuterated chloroform ($CDCl_3$) and (B) deuterated water (D_2O). Figure insets represent magnifications of the aromatic protons from β-lap.

3.2. Solubility of β-lap in PLA polymer

In order to gain insight into interactions between β-lap and the core-forming material (i.e. PLA), solid-state solubility studies were performed using DSC. Values of ΔH_m (J/g) were plotted as a function of β-lap loading percentage (Fig. 2A). The *X*-intercept, provided by linear regression of the data, yields the solid-state solubility of β-lap in PLA at 31%. The dissolution behavior of β-lap within PLA helps to explain discrepancies in drug loading among the different micelle fabrication procedures. Close inspection of images of β-lap/PEG5k–PLA5k films at different loading percentages illustrates the dissolution of drug within the polymer (Fig. 2B). At levels below the solid-state solubility value, the drug and polymer appear as a continuous film. However, at higher loading percentages (20%), β-lap crystals appeared in the film, indicative of drug loading above the solubility threshold of β-lap in PLA core.

3.3. β-Lap micelle characterization

Drug-loaded micelle size was determined utilizing dynamic light scattering (DLS) for each of the fabrication methods examined (Table 1). The three different methods all produced micelles of an adequate size (e.g. 10–100 nm), with the dialysis and solvent evaporation procedures yielding micelle sizes of 23.3±1.2 nm and 17.3±0.2 nm, respectively. The film sonication procedure produced micelles with a slightly greater average diameter (29.6±1.5 nm), possibly due to the increased loading of the drug within the micelle core [32].

Encapsulation of β-lap inside micelle cores was demonstrated by comparing ^{1}H NMR spectra of micelle samples in deuterated chloroform ($CDCl_3$) and deuterated water (D_2O) (Fig. 3). In $CDCl_3$, prominent resonance peaks of β-lap were observed in addition to those of PLA and PEG blocks, indicating that the micelle contains both copolymer and β-lap. In contrast, only the PEG resonance peaks were detected in D_2O, while both the PLA and β-lap resonance peaks were absent. The micelle shells consisting of PEG blocks were well solvated in D_2O and therefore showed clear ^{1}H NMR signal. In contrast, when β-lap was encapsulated inside micelle cores,

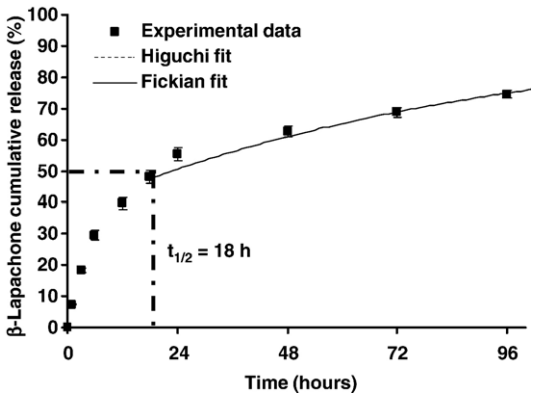

Fig. 4. In vitro β-lap release profiles from PEG–PLA polymer micelles in PBS at pH 7.4 and 37 °C. The error bars were calculated as standard deviation from triplicate samples.

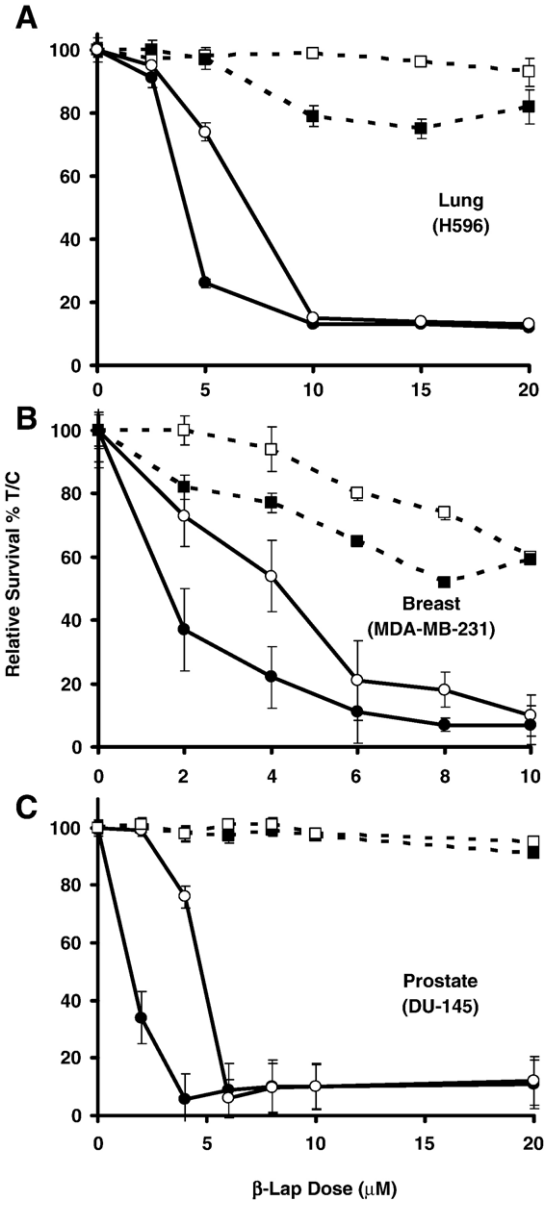

Fig. 5. Long-term, relative survival assays of (A) H596 lung, (B) DU-145 prostate, and (C) MDA-MB-231 breast cancer cells treated with β-lap at indicated doses for 2 h. In the figures, –□– corresponds to NQO1− cells treated with β-lap micelles, –■– represents NQO1− cells treated with free β-lap, –○– corresponds to NQO1+ cells treated with β-lap micelles, and –●– represents NQO1+ cells treated with free drug.

resonance peaks of PLA blocks and β-lap were not observed due to their insufficient mobility in D_2O, consistent with the core-shell structure of polymeric micelles [33,34].

The release kinetics of β-lap from PEG–PLA polymer micelles were examined in vitro (Fig. 4). As can be seen from the figure, the time for 50% of drug release ($t_{1/2}$) is 18 h, with the majority of the drug (~75%) being released over the course of 4 days. Alonso and coworkers have demonstrated that PEG–PLA nanoparticles do not undergo significant degradation over two weeks incubation in PBS buffer (pH 7.4) at 37 °C [35,36]. Based on these and other findings, drug is released primarily via diffusion processes, and was modeled as such. Simulated model drug release is shown along with experimentally measured cumulative release data. The Higuchi based model [23] output was successfully fit to the experimental measurements from 0–18 h. D_h had an estimated value of 4.2×10^{-17} cm^2/s (95% confidence interval: $4.0–4.4\times10^{-17}$ cm^2/s). After 18 h, the Fickian [24,25] diffusion approximation begins to fit the data and continues to fit the data until the end of the study. For the Fick approximation, the value of diffusion, D_f, is 2.3×10^{-19} cm^2/s (95% confidence interval: $2.0–2.5\times10^{-19}$ cm^2/s), almost 200 times slower than drug transport for the first 18 h. The quality of the model fits and low error of the parameter estimates indicate that both models well approximate the drug release data at different times of drug release. However, the diffusion rates at each stage of drug release differed considerably, suggesting that two different processes may be taking place. In the first 18 h, drug release occurs relatively quickly through a Higuchi-like mechanism. Drug released in this period of time could be precipitated in and around the micelle core but may have good access to the surrounding aqueous environment through micelle surface. However, diffusion after 18 h is dramatically slower, which may reflect drug that has less access to the surrounding hydrophilic corona. This fraction of the drug loading could be entrapped in or even dissolved in dense solid regions of the hydrophobic core, where polymer entanglement serves as a much greater impediment to drug transport.

3.4. Mechanism of action of cell death induced by β-lap micelles

Growth assays were performed to examine the mechanism of action of β-lap micelles on NQO1-overexpressing tumor cells compared to NQO1-null tumor cells. NQO1− cells also serve to mimic normal tissues that are NQO1 deficient. Fig. 5 depicts relative survival curves (%T/C) in vitro of three different tumor cell lines (lung, prostate, and breast) treated with free β-lap and β-lap micelles at different drug doses. Results show that after a 2 h incubation with β-lap micelles, a significant increase in cytotoxicity can be observed in NQO1+ over NQO1− cells in all three cell lines. In H596 cells, a 26% loss in survival in NQO1+ cells following 5 μM β-lap micelle administration was noted, and at 10 μM an approximate 85% loss in survival was observed. Values for β-lap micelles were consistently less cytotoxic than for free drug exposures. β-Lap micelle cytotoxicity was equal to that of free β-lap drug administration at 10 μM, with the difference in cytotoxicities at smaller doses attributed to a delay in drug release from the micelles. Finally, while free β-lap leads to an approximate 25% loss in survival in NQO1− cells at a 15 μM dose, β-lap micelles have minimal toxicity in NQO1− cells (~7% loss in survival at 20 μM dose).

The same pattern of cell cytotoxicity for the NQO1+ cells and survival in the NQO1− cells was evident in human prostate and breast cancer cells. In DU-145 and MDA-MB-231 cells, β-lap micelles killed more than 50% of NQO1+ cells at a dose of 6 μM. At further dose increases, β-lap micelle cytotoxicity approached that of free β-lap. NQO1− cells were resistant to β-lap micelles. In DU-145 cells, there was less than a 10% loss in

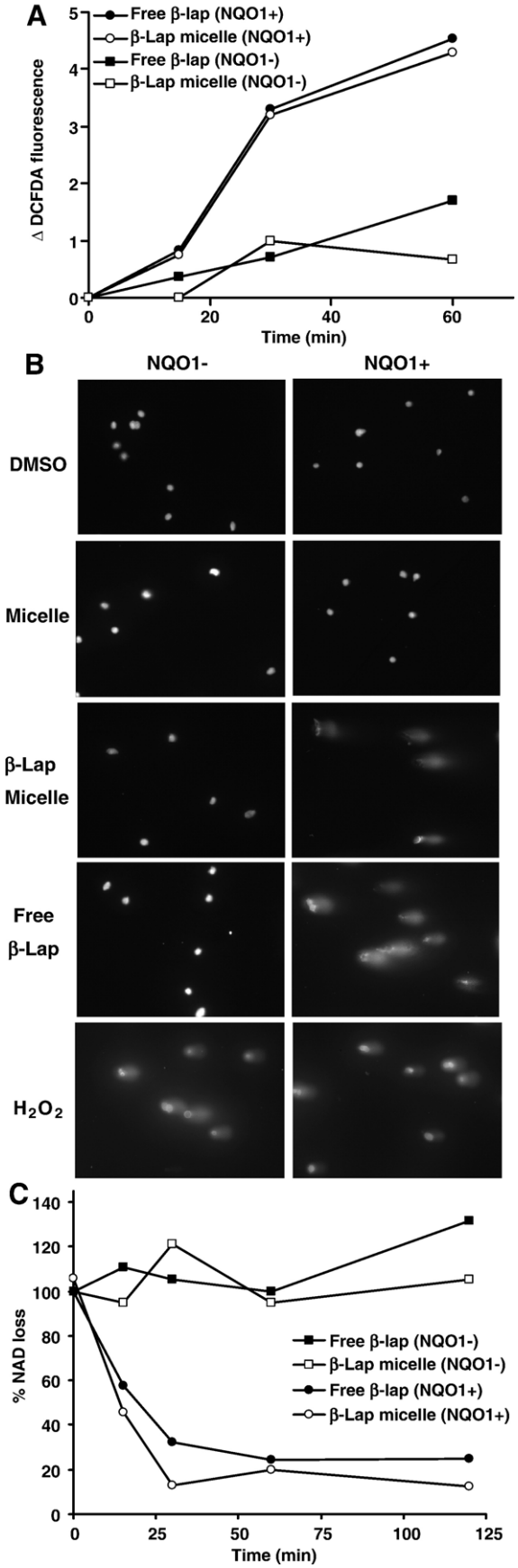

cell survival after coadministration of dicoumarol (NQO1 inhibitor) with β-lap micelles. Similarly, NQO1− MDA-MB-231 cells were resistant to β-lap micelles. Importantly drug-free micelles were shown to have no cytotoxic effect on tumor cells (data not shown).

In attempts to elucidate whether the unique mechanism of action of β-lap was preserved through micellar delivery of the drug, several key biological assays were performed in H596 cells to identify vital components of β-lap-mediated cell death in NSCLC, as reported by Bey et al. [26]. Fig. 6 shows the results of the three biological assays (ROS analysis, comet assays, and NAD loss) conducted to examine vital characteristics of β-lap-induced cell death. Administration of β-lap micelles at a dose of 10 μM leads to oxidative stress in NQO1+ cells in a manner identical to that of free β-lap drug administration. In contrast, β-lap-induced oxidative stress was absent in NQO1− cells. In the NQO1− cells, no DNA damage was evident after exposure with free β-lap drug or β-lap micelles. However, in the NQO1+ cells, extensive comet tail formation can be observed, indicating DNA damage. Lastly, Fig. 6C shows NAD loss associated with β-lap micelle administration to H596 cells at the 10 μM dose. As can be observed from the figure, no NAD loss occurs in the NQO1− cells, while an exponential decrease in NAD is observed with increasing time of exposure to micelles. Taken together, these results serve to show that the unique mechanism of action of β-lap is preserved through micellar delivery.

4. Discussion

The objective of the present study was to develop polymer micelles that can effectively encapsulate β-lap with adequate loading density and minimal loss of drug and polymer. Of the three methods examined in this study, film sonication yielded micelles with the highest loading density and loading efficiency. The dialysis method has been shown to be effective in cases where the encapsulated agent is very water insoluble. Despite the low water solubility (0.04 mg/mL) of β-lap, this value is still much higher compared to agents such as paclitaxel (0.34 μg/mL) [37]. Hence, the majority of β-lap can still be lost to the surrounding aqueous medium during dialysis, leaving only a very minimal amount (0.02±0.01%) within the micelles. The solvent evaporation technique is another widely used method for micelle formation, and we have successfully formed PEG–PLA polymer micelles with high doxorubicin loading [38]. However, this method also proved inefficient at loading β-lap within micelles (loading density=0.39±0.05%), mainly because of the crystallization behavior of β-lap. Both the dialysis and solvent evaporation methods have slow processes of

Fig. 6. Cell death and DNA damage assays conducted in NQO1+ and NQO1− H596 NSCLC cells at a dose of 10 μM of free β-lap or β-lap-containing micelles. (A) Induction of ROS in H596 cells incubated for 20 min with CM-H_2DCFDA and then treated with the dose and assessed at the times indicated. (B) Alkaline comet assays of H596 following a 2 h exposure. Vehicle alone (DMSO), micelles alone, and H_2O_2 (for NQO1 independent DNA damage) served as controls. (C) Nucleotide loss following exposure and assessed at the times indicated.

micellar formation, requiring time for organic solvent to exchange with an aqueous environment or evaporate organic solvent, respectively. In contrast, β-lap crystallization is a faster kinetic process, which can result in the loss of the majority of drug to crystal formation.

The film sonication method proved effective at achieving higher drug loading density within micelles. This increased loading can be best explained by the formation of a molecular level mixture between β-lap and PLA. During the film formation process, β-lap dissolves within the PLA core at a solid-state solubility of 31% (Fig. 2A). At values below this limit, β-lap forms a homogeneous molecular-level mixture with the PLA matrix. The dissolution of drug within the polymer matrix prevents β-lap from crystallizing during micelle formation, leading to higher drug loading density within the micelles. Similar phenomenon was observed previously by Panyam et al. where an increase in drug loading correlated with increases in solid-state solubility [20]. While the film sonication method led to a significant increase in drug loading density, the loading efficiency was only approximately 40%. We hypothesize that β-lap mixed with PEG chains in the film may not be efficiently loaded inside the micelle core upon sonication. One possible strategy to overcome this limitation is to use longer core forming blocks as demonstrated by Allen et al. [39], or the addition of PLA within the film.

The film sonication method leads to micelles with an increased amount of β-lap encapsulated within the core (4.7± 1.0% to 6.5±1.0%). Additionally, the hydrodynamic diameter of the micelles (29.6±1.5 nm) as measured by DLS also proves adequate for future in vivo delivery applications. Micelles of similar diameters (e.g. SP1049C and Genexol) have shown prolonged blood circulation times [40]. ^{1}H NMR studies clearly demonstrated the core-shell structure of the polymer micelles produced by the film sonication procedure. The results indicate that the drug is encapsulated within the PLA micelle core and the micelle surface is stabilized with a mobile PEG corona. Such core-shell structure has the potential advantage in the protection of the drug from enzymatic degradation while the PEG layer hinders plasma protein adsorptions and particle aggregation. Gref et al. found that reduced protein adsorption depended greatly on PEG molecular weight (~5000 Da) and density at the surface (~2–5%) [41]. In a different study, Hsiue and coworkers found that PEG–PLA micelles were stable in bovine serum albumin (BSA) for incubation timepoints of up to 25 h, as evidenced by minimal change of particle size [42]. Reduction in plasma protein interaction should translate into very stable micelles following IV injection, as shown by Kataoka and coworkers, who demonstrated that 25% of injected PEG–PLA micelles were found to be stably circulating in blood vessels 24 h after injection [43]. The aforementioned Genexol®, a paclitaxel-containing PEG–PLA micelle formulation currently in phase I clinical trials, was shown by Bang and coworkers to have a blood elimination half-life of approximately 11 h. This same study showed that the micelle formulation had significant increase in MTD, and improved antitumor efficacy when compared to a traditional paclitaxel formulation, consistent with stable drug encapsulation in micelles in vivo [44].

In vitro growth inhibition assays demonstrate that β-lap micelles effectively kill a variety of tumor cells overexpressing NQO1 while sparing NQO1− cells. Close examination shows that micelle-delivered β-lap is less toxic to both NQO1+ and NQO1− cells compared to the free drug (Fig. 5). Several reasons may explain this discrepancy. Firstly, the actual intracellular concentration of β-lap may be smaller in cells incubated with β-lap micelles than those with free drug. This is possible since most anticancer agents are lipophilic (as well as hydrophobic) and can easily cross cell membranes. PEG-stabilized nanoparticles are typically internalized through fluidic phase endocytosis [14], and PEG shielding can effectively reduce cell uptake, leading to a smaller drug concentration inside the cells. Secondly, after cell internalization, micelle-delivered β-lap may not be immediately available due to micelle encapsulation. In vitro drug release studies showed the value of $t_{1/2}$ is 18 h (Fig. 4). This delayed drug availability may also contribute to a lesser cytotoxicity as shown in both NQO1+ and NQO1− cells. Despite reduced in vitro toxicity, the value of β-lap micelles will likely result in the increased drug solubility and improved pharmacokinetics over free drug during in vivo applications. In polymer–drug conjugate systems developed by Li et al. [45] and Ulbrich et al. [46] for the delivery of paclitaxel and doxorubicin respectively, the conjugated drugs showed less in vitro cytotoxicity compared to the free drugs, however, their antitumor efficacy responses were considerably higher due to increased accumulation in tumors.

Comprehensive biological studies show that the unique mechanism of action of β-lap, as shown previously by Bey et al. [26] is preserved through micellar drug delivery. In NQO1-overexpressing tumor cells incubated with β-lap micelles, reactive oxygen species (ROS) were generated (Fig. 6A) as a result of NQO1-dependent futile cycling of the β-lap and subsequent depletion of NAD(P)H from the cell (Fig. 6C). Accumulation of ROS such as hydroxyl radicals causes massive DNA damage as shown in comet assay for β-lap micelles as well as the free drug (Fig. 6B). This NQO1-specific cytotoxicity combined with micellar drug delivery bodes well for in vivo translation of the platform, where upon administration, β-lap micelles will accumulate in tumor tissue through passive targeting and release β-lap, which will only be bioactivated in the presence of high levels of NQO1. Concurrently, normal healthy tissues will be spared from the cytotoxic effect of β-lap due to lack of NQO1 expression and reduced micelle uptake.

5. Conclusions

In summary, we have successfully developed β-lap-PEG–PLA polymer micelles with adequate loading density, optimal size, core-shell structure, and diffusion-based release kinetics. Upon administration to NQO1+ and NQO1− cells, we were able to show an NQO1-dependent cytotoxicity that resembles that of free drug administration, where NQO1+ cells are effectively killed and NQO1− cells are spared. Future studies will focus on the preclinical evaluation of these micelles in NQO1-overexpressing animal tumor models.

Acknowledgements

This work was supported by an NIH grant CA90696 to JG, NIH grant CA102792 to DAB, and DOD grant W81XWH-04-1-0164 to DAB. EB is grateful for the support of a National Institutes of Health minority supplement grant. This is report CSCNP10 from the Program in Cell Stress and Cancer Nanomedicine at UT Southwestern Medical Center at Dallas.

References

[1] M. Belinsky, A.K. Jaiswal, NAD(P)H:quinone oxidoreductase1 (DT-diaphorase) expression in normal and tumor tissues, Cancer Metastasis Rev. 12 (2) (1993) 103–117.
[2] C.D. Logsdon, D.M. Simeone, C. Binkley, T. Arumugam, J.K. Greenson, T.J. Giordano, D.E. Misek, R. Kuick, S. Hanash, Molecular profiling of pancreatic adenocarcinoma and chronic pancreatitis identifies multiple genes differentially regulated in pancreatic cancer, Cancer Res. 63 (10) (2003) 2649–2657.
[3] A.M. Lewis, M. Ough, J. Du, M.S. Tsao, L.W. Oberley, J.J. Cullen, Targeting NAD(P)H:Quinone oxidoreductase (NQO1) in pancreatic cancer, Mol. Carcinog. 43 (4) (2005) 215–224.
[4] D. Siegel, D. Ross, Immunodetection of NAD(P)H:quinone oxidoreductase 1 (NQO1) in human tissues, Free Radic. Biol. Med. 29 (3–4) (2000) 246–253.
[5] J.J. Pink, S.M. Planchon, C. Tagliarino, M.E. Varnes, D. Siegel, D.A. Boothman, NAD(P)H:Quinone oxidoreductase activity is the principal determinant of beta-lapachone cytotoxicity, J. Biol. Chem. 275 (8) (2000) 5416–5424.
[6] C. Tagliarino, J.J. Pink, G.R. Dubyak, A.L. Nieminen, D.A. Boothman, Calcium is a key signaling molecule in beta-lapachone-mediated cell death, J. Biol. Chem. 276 (22) (2001) 19150–19159.
[7] K.E. Reinicke, E.A. Bey, M.S. Bentle, J.J. Pink, S.T. Ingalls, C.L. Hoppel, R.I. Misico, G.M. Arzac, G. Burton, W.G. Bornmann, D. Sutton, J. Gao, D.A. Boothman, Development of beta-lapachone prodrugs for therapy against human cancer cells with elevated NAD(P)H:quinone oxidoreductase 1 levels, Clin. Cancer Res. 11 (8) (2005) 3055–3064.
[8] M. Ough, A. Lewis, E.A. Bey, J. Gao, J.M. Ritchie, W. Bornmann, D.A. Boothman, L.W. Oberley, J.J. Cullen, Efficacy of beta-lapachone in pancreatic cancer treatment: exploiting the novel, therapeutic target NQO1, Cancer Biother. 4 (1) (2005) 95–102.
[9] N. Nasongkla, A.F. Wiedmann, A. Bruening, M. Beman, D. Ray, W.G. Bornmann, D.A. Boothman, J. Gao, Enhancement of solubility and bioavailability of beta-lapachone using cyclodextrin inclusion complexes, Pharm. Res. 20 (10) (2003) 1626–1633.
[10] G.S. Kwon, M.L. Forrest, Amphiphilic block copolymer micelles for nanoscale drug delivery, Drug Dev. Res. 67 (1) (2006) 15–22.
[11] H. Otsuka, Y. Nagasaki, K. Kataoka, PEGylated nanoparticles for biological and pharmaceutical applications, Adv. Drug Deliv. Rev. 55 (3) (2003) 403–419.
[12] V.P. Torchilin, Micellar nanocarriers: pharmaceutical perspectives, Pharm. Res. 24 (1) (2007) 1–16.
[13] M. Jones, J. Leroux, Polymeric micelles — a new generation of colloidal drug carriers, Eur. J. Pharm. Biopharm. 48 (2) (1999) 101–111.
[14] R. Savic, L. Luo, A. Eisenberg, D. Maysinger, Micellar nanocontainers distribute to defined cytoplasmic organelles, Science 300 (5619) (2003) 615–618.
[15] V.P. Torchilin, A.N. Lukyanov, Z. Gao, B. Papahadjopoulos-Sternberg, Immunomicelles: targeted pharmaceutical carriers for poorly soluble drugs, Proc. Natl. Acad. Sci. U. S. A. 100 (10) (2003) 6039–6044.
[16] H. Hashizume, P. Baluk, S. Morikawa, J.W. McLean, G. Thurston, S. Roberge, R.K. Jain, D.M. McDonald, Openings between defective endothelial cells explain tumor vessel leakiness, Am. J. Pathol. 156 (4) (2000) 1363–1380.
[17] H. Maeda, The enhanced permeability and retention (EPR) effect in tumor vasculature: the key role of tumor-selective macromolecular drug targeting, Adv. Enzyme Regul. 41 (2001) 189–207.
[18] S.M. Planchon, S. Wuerzberger, B. Frydman, D.T. Witiak, P. Hutson, D.R. Church, G. Wilding, D.A. Boothman, Beta-lapachone-mediated apoptosis in human promyelocytic leukemia (HL-60) and human prostate cancer cells: a p53-independent response, Cancer Res. 55 (17) (1995) 3706–3711.
[19] X. Shuai, H. Ai, N. Nasongkla, S. Kim, J. Gao, Micellar carriers based on block copolymers of poly(epsilon-caprolactone) and poly(ethylene glycol) for doxorubicin delivery, J. Control. Release 98 (3) (2004) 415–426.
[20] J. Panyam, D. Williams, A. Dash, D. Leslie-Pelecky, V. Labhasetwar, Solid-state solubility influences encapsulation and release of hydrophobic drugs from PLGA/PLA nanoparticles, J. Pharm. Sci.-Us 93 (7) (2004) 1804–1814.
[21] F.J. Wang, E. Blanco, H. Ai, D.A. Boothman, J. Gao, Modulating beta-lapachone release from polymer millirods through cyclodextrin complexation, J. Pharm. Sci.-Us 95 (10) (2006) 2309–2319.
[22] D. Sutton, S. Wang, N. Nasongkla, E. Dormidontova, J. Gao, Doxorubicin and beta-lapachone release and interaction with micellar core materials. Exp. Biol. Med. (in press).
[23] T. Higuchi, Mechanism of sustained-action medication. Theoretical analysis of rate of release of solid drugs dispersed in solid matrices, J. Pharm. Sci. 52 (1963) 1145–1149.
[24] J. Crank, The Mathematics of Diffusion, Oxford University Press, New York, NY, 1975.
[25] P.L. Ritger, N.A. Peppas, A simple equation for description of solute release I. Fickian and non-fickian release from non-swellable devices in the form of slabs, spheres, cylinders or discs, J. Control. Release 5 (1) (1987) 23–36.
[26] E.A. Bey, M.S. Bentle, K.E. Reinicke, Y. Dong, C.R. Yang, L. Girard, J.D. Minna, W.G. Bornmann, J. Gao, D.A. Boothman, A novel NQO1-and PARP-1-mediated cell death pathway induced in non-small cell lung cancer cells by beta-lapachone. Proc. Natl. Acad. Sci. U. S. A. (in press).
[27] C. Labarca, K. Paigen, A simple, rapid, and sensitive DNA assay procedure, Anal. Biochem. 102 (2) (1980) 344–352.
[28] M.S. Bentle, K.E. Reinicke, E.A. Bey, D.R. Spitz, D.A. Boothman, Calcium-dependent modulation of poly(ADP-ribose) polymerase-1 alters cellular metabolism and DNA repair, J. Biol. Chem. 281 (44) (2006) 33684–33696.
[29] C. Tagliarino, J.J. Pink, K.E. Reinicke, S.M. Simmers, S.M. Wuerzberger-Davis, D.A. Boothman, Mu-calpain activation in beta-lapachone-mediated apoptosis, Cancer Biother. 2 (2) (2003) 141–152.
[30] V. Panduri, S.A. Weitzman, N.S. Chandel, D.W. Kamp, Mitochondrial-derived free radicals mediate asbestos-induced alveolar epithelial cell apoptosis, Am. J. Physiol., Lung Cell. Mol. Physiol. 286 (6) (2004) L1220–L1227.
[31] P.L. Olive, J.P. Banath, R.E. Durand, Heterogeneity in radiation-induced DNA damage and repair in tumor and normal cells measured using the "comet" assay, Radiat. Res. 122 (1) (1990) 86–94.
[32] V.P. Torchilin, Targeted polymeric micelles for delivery of poorly soluble drugs, Cell. Mol. Life Sci. 61 (19–20) (2004) 2549–2559.
[33] C.R. Heald, S. Stolnik, K.S. Kujawinski, C. De Matteis, M.C. Garnett, L. Illum, S.S. Davis, S.C. Purkiss, R.J. Barlow, P.R. Gellert, Poly(lactic acid)–poly(ethylene oxide) (PLA–PEG) nanoparticles: NMR studies of the central solidlike PLA core and the liquid PEG corona, Langmuir 18 (9) (2002) 3669–3675.
[34] J.S. Hrkach, M.T. Peracchia, A. Domb, N. Lotan, R. Langer, Nanotechnology for biomaterials engineering: structural characterization of amphiphilic polymeric nanoparticles by H-1 NMR spectroscopy, Biomaterials 18 (1) (1997) 27–30.
[35] R. Gref, P. Quellec, A. Sanchez, P. Calvo, E. Dellacherie, M.J. Alonso, Development and characterization of CyA-loaded poly(lactic acid)–poly (ethylene glycol)PEG micro- and nanoparticles. Comparison with conventional PLA particulate carriers, Eur. J. Pharm. Biopharm. 51 (2) (2001) 111–118.
[36] P. Quellec, R. Gref, E. Dellacherie, F. Sommer, M.D. Tran, M.J. Alonso, Protein encapsulation within poly(ethylene glycol)-coated nanospheres. II.

Controlled release properties, J. Biomed. Mater. Res. 47 (3) (1999) 388–395.
[37] W. Bouquet, W. Ceelen, B. Fritzinger, P. Pattyn, M. Peeters, J.P. Remon, C. Vervaet, Paclitaxel/beta-cyclodextrin complexes for hyperthermic peritoneal perfusion — formulation and stability, Eur. J. Pharm. Biopharm. (in press), doi:10.1016/j.ejpb.2006.11.025.
[38] N. Nasongkla, E. Bey, J. Ren, H. Ai, C. Khemtong, J.S. Guthi, S.F. Chin, A.D. Sherry, D.A. Boothman, J. Gao, Multifunctional polymeric micelles as cancer-targeted, MRI-ultrasensitive drug delivery systems, Nano Lett. 6 (11) (2006) 2427–2430.
[39] C. Allen, D. Maysinger, A. Eisenberg, Nano-engineering block copolymer aggregates for drug delivery, Colloids Surf., B Biointerfaces 16 (1–4) (1999) 3–27.
[40] D. Sutton, N. Nasongkla, E. Blanco, J. Gao, Functionalized micellar systems for cancer targeted drug delivery. Pharm. Res. (in press), doi:10.1007/S11095-006-9223-y.
[41] R. Gref, M. Luck, P. Quellec, M. Marchand, E. Dellacherie, S. Harnisch, T. Blunk, R.H. Muller, 'Stealth' corona-core nanoparticles surface modified by polyethylene glycol (PEG): influences of the corona (PEG chain length and surface density) and of the core composition on phagocytic uptake and plasma protein adsorption, Colloids Surf., B Biointerfaces 18 (3–4) (2000) 301–313.
[42] C.L. Lo, C.K. Huang, K.M. Lin, G.H. Hsiue, Mixed micelles formed from graft and diblock copolymers for application in intracellular drug delivery, Biomaterials 28 (6) (2007) 1225–1235.
[43] Y. Yamamoto, Y. Nagasaki, Y. Kato, Y. Sugiyama, K. Kataoka, Long-circulating poly(ethylene glycol)–poly(D,L-lactide) block copolymer micelles with modulated surface charge, J. Control. Release 77 (1–2) (2001) 27–38.
[44] T.Y. Kim, D.W. Kim, J.Y. Chung, S.G. Shin, S.C. Kim, D.S. Heo, N.K. Kim, Y.J. Bang, Phase I and pharmacokinetic study of Genexol-PM, a cremophor-free, polymeric micelle-formulated paclitaxel, in patients with advanced malignancies, Clin. Cancer Res. 10 (11) (2004) 3708–3716.
[45] C. Li, D.F. Yu, R.A. Newman, F. Cabral, L.C. Stephens, N. Hunter, L. Milas, S. Wallace, Complete regression of well-established tumors using a novel water-soluble poly(L-glutamic acid) paclitaxel conjugate, Cancer Res. 58 (11) (1998) 2404–2409.
[46] K. Ulbrich, T. Etrych, P. Chytil, M. Jelinkova, B. Rihova, HPMA copolymers with pH-controlled release of doxorubicin — in vitro cytotoxicity and in vivo antitumor activity, J. Control. Release 87 (1–3) (2003) 33–47.